

THE DEGRADATION OF THE BRIDGE DECK SLABS IN BELGIUM MAINLY INVOLVES ALKALI-AGGREGATE REACTIONS

Philippe DEMARS^{1,*}, Pierre GILLES¹, Eric DONDONNE¹, Guy LEFEBVRE²,
Anne DARIMONT³, Gabriel LORENZI⁴, Guy HENRIET⁵, Anne-Marie MARION⁶

¹ Ministère de l'Équipement et des Transports - Direction de l'Expertise des Structures
Rue Côte d'Or 253, B-4000 LIEGE, Belgique

² Ministère de l'Équipement et des Transports - Direction des Structures Routières
Rue de l'Industrie 27, B-1400 NIVELLES, Belgique

³ Université de Liège - Laboratoire des Matériaux de Construction
Sart Tilman – Bâtiment B52, B-4000 LIEGE, Belgique

⁴ Institut scientifique de service public
Rue du Chéra 200, B-4000 LIEGE, Belgique

⁵ Université catholique de Louvain - Laboratoire du Génie Civil
Place du Levant 1, B-1348 LOUVAIN-LA-NEUVE, Belgique

⁶ scientific advisor, B-1190 BRUXELLES, Belgique

Abstract

Since 1995, serious concrete deterioration has been observed in more than 70 bridges in the Walloon Region in Belgium. This new phenomenon locally named “decay of the deck slabs” undergoes different stages of evolution, which may ultimately lead to perforation of the deck slab.

Seven bridges, located in different regions, have been investigated in detail (chemical analysis, physical measurements, concrete petrography and scanning electron microscope observations).

The results showed that the concrete deterioration was due to several simultaneous deleterious processes: alkali-aggregate reactions, chloride attack and freeze-thaw action. Secondary ettringite deposits were also present but without any associated sulfate attack. Occasional calcium chloroaluminate crystals have also been detected in voids. The high alkali content measured comes from the cement and the external de-icing salts. The study also shows that alkalis have migrated from the upper to the lower part of the slab leading to the realkalinisation of the carbonated lower surface.

Keywords: concrete deck slab decay, alkali-aggregate reaction, planar cracking, re-alkalinisation, calcium chloroaluminate.

1 INTRODUCTION

A new kind of concrete deterioration of the bridge deck slabs has been observed since 1995: it is unusual with regards to the known deterioration phenomena such as steel bars corrosion and carbonation. More than 70 bridges are affected by this serious form of damage in the Walloon Region in Belgium : the majority of these bridges are beam bridges (Figure 1). Traversing from its lower to its upper face, the decks in these bridges were composed of a concrete slab of about 18 cm thickness, a waterproofing layer, a protection layer and an asphaltic top cover. Air entrainment was never used within these concretes because of the associated important drop of the compression strength as a consequence of the presence of a lot of air bubbles [1].

This phenomenon has locally been named “decay of the deck slabs” and presents different stages of evolution as shown by the following macroscopic observations: small to large white or dark patches on the lower face of the deck (whatever the moisture environment may be) (Figure 2); planar cracking with whitish deposits (specifically observed on the drilling cores – Figure 3); crumbling of the concrete into a gravel consistency on the upper surface of the deck (“potholes”) and ultimately the perforation of the deck (Figure 4).

All these phenomena are firstly due to defects in the waterproofing [2].

To try to understand the deterioration mechanism involved, seven bridges (shortly referred to as b, h, l, r, w and f) have been investigated in detail; they were located in regions differing in their climatic and geological environments. The aim was to find concretes specifically with and without

alkali-reactive aggregates. Various laboratory techniques were performed as well on the so called “sound concretes” as well as on the concretes showing deterioration. Cores have been drilled in both area types with or without coloured patches.

2 METHODS

Tests were carried out on cores of 50 and 80 mm diameter size, drilled in both zones with and without the coloured patches, to try to distinguish between the supposed sound concrete and the deteriorated concrete.

The following chemical, physical and mechanical tests were performed : depth of carbonation measurement (EN 14630), cement content (NBN B15-250), sulphate content (NBN B15-256), chlorides content (NBN B15-257 and NBN T61-201), alkali content (warm acid attack) by atomic absorption, water absorption after immersion (NBN B15-215), vacuum water absorption (NBN B15-213), tensile strength (NBN B15-211 and EN 1542), compressive strength (NBN B15-220), static and dynamic permeabilities, ultrasonic velocity, petrographic analysis on thin sections and scanning electron microscope (SEM) coupled with an EDX analyser.

The measurement of the vertical and horizontal ultrasonic velocities (NBN B15-229) was also performed by direct transmission through the cores with pointed transducers.

The freeze-thaw resistance assessment was performed according to NBN B15-231 with ultrasonic velocity measurement after every cycle.

The static and dynamic permeabilities were performed on samples of 80 mm height and 80 mm diameter taken from the concrete cores, outside the planar cracking. Several samples were drilled horizontally from 113 mm diameter vertical cores; the static permeability was measured with a constant water level; the pressure difference was 0.1-0.2 MPa. The dynamic permeability was measured under a cyclic compression stress (frequency : 0.33 Hz - 0.01 to 1.56 MPa).

Petrography was also carried out on thin sections of 25 microns thickness cut perpendicular to the slab surface, from cores split in two parts ; the second part being used for chemical analysis.

In addition observations under the SEM with EDX were carried out on the planar cracking surface and on the breaking-down surface after the tensile strength test.

Some of the analytical methods have been adapted during the research : e.g. in the beginning, the chemical analysis were carried out on entire cores; the sampling had to be adapted by splitting the core into multiple slices of a few millimetres thickness each. This method revealed physical and chemical vertical changes with depth through the cores. Petrography was also only undertaken on the upper and lower parts of the cores. Later, more detailed results were obtained by analysing the whole core.

3 RESULTS

3.1 Mechanical, physical and chemical tests

The analysis of the results, summarized at Table 1, allows following conclusions.

The tensile strength was weak ($<2 \text{ N/mm}^2$) with sometimes values equal to zero in the upper part of the cores, corresponding to areas of planar cracking.

The immersion water absorption was often greater than 6 %. Immersion and vacuum water absorption values were very closed to each other.

In some cases, the phenolphthalein solution didn't reveal any concrete carbonation (0 mm depth), when this had been already observed by the naked-eye and by petrography, on the lower surface of the slab.

The Na_2O and K_2O contents varied independently of each other.

Chlorides content were detected between 0.01 and 0.53% of concrete weight. The highest values having been measured in the upper slabs surfaces. This may induce severe steel bars corrosion, which was observed only in the crumbling concrete zones on the upper bridge deck face. But outside these zones, corrosion was lower as it can be sometimes observed when concrete is removed by hydro-demolition

Chlorides and alkalis contents showed vertical and horizontal chemical gradients in the slab.

The horizontal permeability was greater than the vertical permeability. The permeability measured under a dynamic vertical stress is lower than under a static vertical stress.

The freeze-thaw resistance was measured only on sound concretes. The results showed high initial ultrasonic velocity (4000 m/s) corresponding to a sound concrete. After freeze-thaw cycles, a drop of ultrasonic velocity is recorded. It is highly variable between 0 to 52 % from one zone to the other of the same bridge.

3.1 Microscopy

Petrography

The petrographic examination provided several interesting observations.

Presence of reactive aggregates in all deteriorated slabs. Aggregate lithologies were identified including phyllitic sandstone, silicified and non-silicified limestone (the latter did not include secondary silica, but very fine reactive detrital microquartz embedded within the clayey matrix) [3] (Figure 5), porphyritic quartz-rich microdiorite and finally porous and non-porous flints.

Two types of cement were observed: Portland cement and a blended cement with a medium content of blast furnace slag, roughly estimated between about 10 and 40 % (Figure 6).

Carbonation depths of up to 20 mm, were observed in all lower faces.

Water-cement ratios were high and varied between 0.50 and 0.70 (Figure 7).

Water additions (retempering) have been revealed by the presence of large water pores and bleeding channels (Figure 8).

Planar cracking were often observed in the upper part of the slabs, connected with transverse cracks (Figure 9).

A good correlation was observed between the degree of cracking and the ASR frequency in the whole cores (Figure 10).

Alkali-silica gels were present in all deteriorated slabs (Figure 11).

Scanning electron microscope

The observation of fracture surfaces revealed several secondary precipitation deposits.

Rims of alkali-silica gel were observed around some of the reactive aggregates (Figure 12). They formed as a combined group of layers (Figure 13) with the layers differing in calcium or potassium contents (Figure 14). Sometimes these layers were recrystallized (Figure 15) in rosette-like minerals.

Secondary ettringite has been frequently found, showing either a needle-like (Figure 16) or sometimes a gel-like habit (Figure 17) in which silica is present as well.

Idiomorphic crystals of calcium chloroaluminate hydrate were present in some voids, in the upper part of the slabs.

4 DISCUSSION

Although the damaged bridges were located in regions differing in their geological environment, all the deteriorated concretes have been attacked by the alkali-silica reaction. This reaction requires an interaction between reactive aggregates, alkali hydroxides from the pore solution and water.

The reactive aggregates participating to the reaction were as follows: phyllitic sandstone, porous and non-porous flints, porphyritic quartz-rich microdiorite, Carboniferous silicified limestone and Devonian non-silicified limestone. These latter reactive rocks were already well-known to be reactive [4]. In regard to the phyllitic sandstone from Southern Belgium, it has been found to be reactive during this research; and its pessimum effect has subsequently been defined later on [5].

The concretes were all composed of either Portland cement or blended cement with a high total alkali content. The amount of slag in the blended cements has been roughly estimated by petrography at between about 10 and 40 %. This content of slag is not high enough to inhibit ASR, as showed in this study. This is in accordance with the opinion generally accepted that the mineral admixtures like slag counteracts the ASR, particularly when the slag replacement is higher than 50 % [6,7].

Defects in the waterproofing allowed water to penetrate into the concrete.

Finally, it was concluded that a relatively good correlation was found between the cracking degree and the ASR frequency in the whole cores.

The planar cracking was not generally considered to be due to the corrosion of the reinforcement steel bars, because it was often observed below and/or above the reinforcement. Moreover, in the more degraded 'crumbling' areas, the reinforcement steel bars could be highly corroded by water and chloride attack, while, outside these zones, corrosion was low as observed after performing hydro-demolition.

There was no evidence of freeze-thaw deterioration. For example, the concrete compositions between the deteriorated and sound concrete in Brigde l was very similar except for aggregate types : in both cases, the aggregates are mid-Devonian limestones quarried out from the same quarry; but the degraded concrete was characterized by the presence of reactive limestone (argillaceous wackestone/packstone) inducing ASR and planar cracking, while the sound concrete contained a non

reactive limestone (sparry boundstone) showing no evidence of ASR and no ASR-induced cracking. If freeze-thaw was mainly acting, a planar cracking should have appeared within the sound concrete as well. On the other hand, no fine cracks have been ever observed within the skin of the upper concrete (chipping) in all the concretes studied. In addition, as formerly underlined, a good correlation was found between the cracking degree and the ASR frequency. With regards to these observations, it seems that the freeze-thaw effect was not necessary the first and/or the main phenomena responsible of the decay of the deck slab, but probably contributed to some extent.

Interpretation

As a result of this study, a mechanism of the deterioration of the bridge deck slabs can be proposed as follows.

In the early stage of its life, the lower surface of the slab was carbonated. When defects appeared in the waterproofing (due to a lack of maintenance, bad work, fatigue, strains, etc...), allowing the fluid circulation, water was then able to get through to the underlying concrete. The heterogeneity in the location of the defects induced a variation in the degree of deterioration in the slab; and this led to a horizontal physico-chemical gradients. When the water percolation passed down the ions through the slab towards its lower part, this led to a vertical physico-chemical gradient.

ASR could develop due to the simultaneous presence of water, alkali-reactive aggregates and a high alkalis content derived from the cement paste. Although the alkali-silica gels were enriched in potassium coming from the cement paste, sodium coming from the de-icing salts were also clearly playing a role within the ASR development [8]. These expansive reactions produced the cracking of the concrete, which might modify the freeze-thaw resistance. In consequence, the system is opening up more and more, allowing increased fluids circulation through the concrete.

In the beginning of the deterioration, the cracks were developing in the upper part of the deck; due to the small thickness of the slab and the strength orientation, cracks propagated in a planar direction.

Sulfates, coming primarily from the cement paste, were dissolved in the circulating water and precipitated in the form of either needle-like secondary ettringite or "ettringite gel". Chlorides, derived from external de-icing salts, partially reacted in the upper part of the slab, with the calcium aluminates to produce idiomorphic calcium chloroaluminate hydrates. As the needle-like secondary ettringite and calcium chloroaluminates hydrates minerals are idiomorphic, they are not considered to induce expansion, while the alkali-silica gel and "ettringite gel" are well known as expansion inducing minerals.[9].

The free alkalis (K, Na) found primarily in the pore solution can pass down through the concrete, leading to a vertical chemical gradient. These alkalis, react with calcium carbonate derived from the carbonation of the cement paste to produce hydrocarbonates. These products led to a pH increasing and to the realkalinization of the lower portion of the slab, which was beforehand fully carbonated [10]. Finally, coloured patches appeared at the lower surface of the slab, as a consequence of these various fluids migration. Their shape is concentrically enlarging with time; and correlated well with an alkali contents gradient, the more severe this gradient, the more deterioration of the slabs was observed to develop.

Tests indicative of the pathology

This research proposes some observations and measurements, which allow the identification of the « decay of the bridges deck slabs ». Indeed, if some of the following characteristics are revealed, the deterioration of the slab is confirmed and the long-term durability potential will decrease:

- Macroscopic observation of the slab :
 - Presence of potholes at the upper surface;
 - Presence of white and grey patches at the lower surface;
- Physical measurements :
 - Water absorption after immersion > 6% weight;
 - Dry density < 2200 kg/m³ ;
 - Ultrasonic velocity < 3000 m/s ;
 - Ultrasonic velocities ratio $V_v/V_h < 1$;
 - Permeability varies from a "1 to 10" factor
- Mechanical measurements :
 - Tensile strength (cohesion) < 2 N/mm²;
- Chemical measurements :
 - [SO₃] > 0,5 % (of the concrete weight);

- [Cl]⁻ > 0,06 % (of the concrete weight);
- [Na₂O_{eq}] > 0,3 % (of the concrete weight);
- Realkalinization of the lower part (previously carbonated);
- Microscopy (petrography and SEM):
 - Numerous sites of ASR development;
 - Other secondary mineral precipitations (ettringite, “ettringite gel”, calcium chloroaluminates hydrates);
 - Planar surface cracking;
 - High water/cement ratio > 0.50.

In the aim of identifying this complex pathology, it is of prime importance to take concrete samples from the deteriorated zones as well as the supposedly sound zones.

5 CONCLUSIONS

Since 1995, a lot of bridges in Belgium have begun to show serious concrete degradation of their deck slab. Macroscopic observations, such as potholes, crumbling of the concrete into a gravel consistency on the upper surface of the deck, the perforation of the deck, and patches at the lower surface of the slabs, all indicated a defect of the waterproofing, leading to the so-named “decay of the deck slabs”. To try to understand the deterioration mechanism involved, seven bridges differing in the climatic and geological environments were studied in detail.

The result of this research showed that several combined deleterious processes were noted. Alkali-silica reaction was observed in all the deteriorated concretes, along with chloride attack and, also possible freeze-thaw action. Additionally most of the concretes have been cast with a relatively high water content. Significant ASR degradation was able to develop because of the use of reactive aggregates, the presence of water due to the waterproofing defects and the high alkali content coming from both the cement and the de-icing salts. As far as the alkalis were concerned, the study showed that they have migrated from the upper to the lower part of the deck, leading to the realkalinization of the lower carbonated concrete surface. Often, the highest chlorides content were found in the upper part of the deck.. Secondary non-deleterious ettringite was also present, in pores and cracks, but no actual sulfate attack has been revealed. However, “ettringite gel” was also sometimes observed, and this could have also contributed to the cracking. Occasional calcium chloroaluminate crystals have been detected in the voids but without any obvious expansion effects. The research showed also that the concrete decay was not due to the corrosion of the reinforcement steel bars, even if corrosion was observed in the upper crumbled concrete.

Moreover, to assess the degree of the deterioration of the concrete slabs, some tests indicative of the pathology have been proposed, such as, water absorption, permeability, ultrasonic velocities and V_v/V_h ratio, cohesiveness, carbonation depth and realkalinization testing, chemical gradient assessments and microscopy allowing to detect the presence of secondary reactions (ASR, ettringite and “ettringite gel”, calcium chloroaluminate hydrates).

6 REFERENCES

- [1] CRR (2002) : Code de bonne pratique pour l'utilisation des entraîneurs d'air dans les bétons routiers – Application, formulation et contrôle. Recommandation R 73/02 :pp 1-42. Centre de Recherches routières, Bruxelles.
- [2] Demars Ph, Gilles P, Dondonne E, Degeimbre R, Darimont A, Lorenzi G, Mertens A (2001) : Dégradation de dalles de tablier de ponts en Belgique - Etude d'une pathologie complexe. Bulletin des laboratoires des Ponts et Chaussées (n° 232) : pp. 73-83.
- [3] Lorenzi G, Guédon S, Antenucci D (2001) : The status of the reactive silica in the limestones susceptible to the alkali-silica reaction (ASR) : contribution of petrographic and SEM techniques. Proceedings of the 8th Euroseminar on microscopy applied to building materials. Athens, Greece, September.
- [4] Lorenzi G, Jensen J, Wigum B, Sibbick R, Haugen M, Guédon S, Åkesson U (2006) : Petrographic atlas of the potentially alkali-reactive rocks in Europe.. Professional paper 2006/1 – N.302. Geological Survey of Belgium.
- [5] Merriaux K, Lecomte A, Degeimbre R, Darimont A (2003) : Alkali-silica reactivity with pessimum content on Devonian aggregates from the Belgian Arden massive. Magazine of Concrete Research, 55, N°5, pp 429-437.
- [6] Swamy R. N. (1992) : The alkali-silica reaction in concrete. Blackie, UK.
- [7] Bérubé M.A., Carles-Gibergues A. (1992). La durabilité des bétons face à l'alkali-réaction, pp 285-350 in La durabilité des bétons. Presses de l'Ecole nationale des Ponts et Chaussées, Paris.

- [8] Grell B (2006) : Experience from testing of the alkali reactivity of european aggregates according to two danish laboratory test methods. Partner report 3.4., Partner project-GRD1-CT-2001-40103, Growth program, European Commission. Sintef report SBF52 A06022, October.
- [9] Pavoine A., Divet L., Fenouillet S., Randazzo V. (2003) : Impact de conditions de cycles de séchage et d'humidification sur la formation différée d'ettringite dans les bétons. Materials and structures/Matériaux et Constructions, vol. 36, novembre 2003, pp 587-593.
- [10] Darimont A, Degeimbre R, Gilles P, Dondonné E, Demars Ph, Mertens de Wilmars A, Lorenzi G, Lefebvre G (2006) : Réalcalinisation du béton carbonaté par migration des alcalins. BLPC, n°261, pp 121-130, avril-mai-juin.

TABLE 1 - Results from mechanical, physical and chemical tests.

Characteristics	Minimum value	Maximum value
Compressive strength, N/mm ²	20-30	50-70
Tensile strength, N/mm ²	0	2
Density (at 105°C), kg/m ³	2100	2300
Water absorption after immersion, % weight	5	8
Vacuum water absorption, % weight	6	9
permeability, 10 ⁻¹⁰ m/s	0.001	16.000
Vertical ultrasonic velocity, m/s	2000	4000
Horizontal ultrasonic velocity, m/s	2500	4200
Vv/Vh	0.63	1.07
Freeze-thaw (only on sound concretes)		
Initial ultrasonic velocity, m/s	3900	4400
Velocity decrease after test, %	0	52
Carbonation depth , mm	0	15
Cement content, kg/m ³	300	400
Alkalies content, % of concrete weight		
K ₂ O	0.05	1.04
Na ₂ O	0.02	0.45
Sulphates contents, % of concrete weight	0.2	1.2
Chlorides contents, % of concrete weight	0.01	0.53



Figure 1: view of a bridge showing the “decay of the deck slabs” phenomenon.



Figure 2: example of a typical patch on the lower surface of a bridge slab.



Figure 3: concrete core drilled through a deck slab and showing a severe delamination.



Figure 4: Perforation of a bridge deck slab.



Figure 5: ASR with a non-silicified Devonian limestone. Alkali-silica gel is observed infilling the crack.
Plane polarized light.

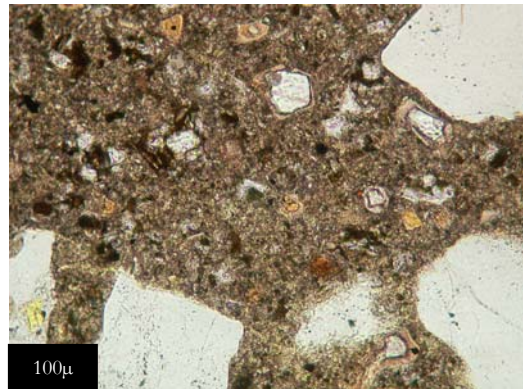


Figure 6: blended Portland cement with a medium content of slag ; clinker relics are also observed.
Plane polarized light.

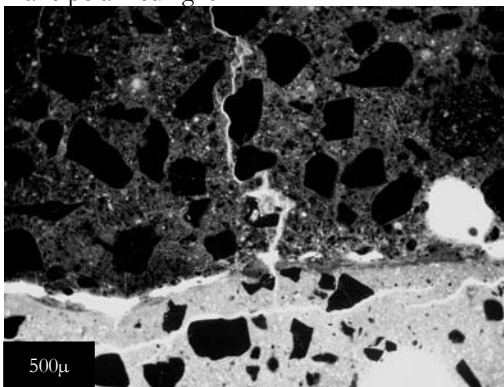


Figure 7: interface between the upper concrete and the lower concrete of a slab : W/C ratio of the lower part is very high. Planar and transverse cracking is observed.
Fluorescent light.

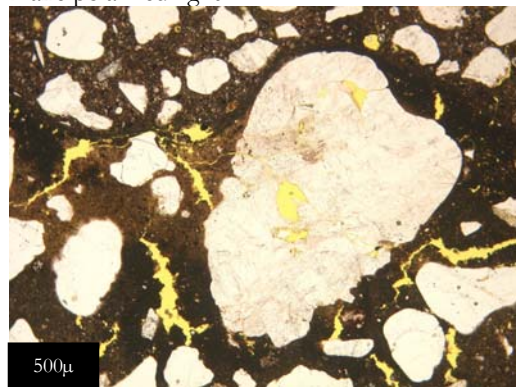


Figure 8: presence of a lot of water pores located within the lower concrete of a slab.
Plane polarized light.

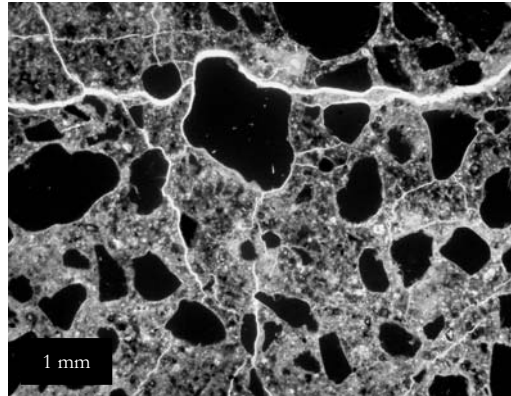


Figure 9: high density of planar and transverse cracks. Fluorescent light.

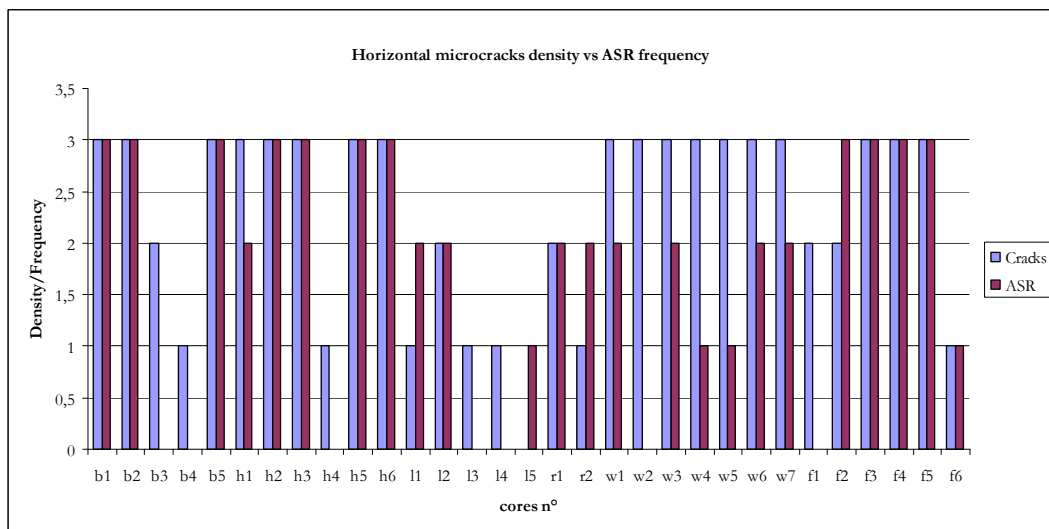


Figure 10: Correlation between the planar micro-cracking degree and the ASR frequency measured on thin sections from concrete cores.

The different bridges are quoted by a letter (b, h, l, r, w and f)

F: Degree of planar micro-cracking determined by semi-quantification and comparison (1 : low, 2 : medium, 3 : severe). ASR density is determined by the number of signs (or sites) of reaction (reactive aggregate, silica gel in pores/cracks (1 to 2 sites = 1; 3 to 5 sites = 2; > 5 sites = 3).

In all cases, when the ASR was present, planar cracking was observed at nearly the same proportion, except for the core L5 in which the ASR was present without any planar micro-cracking. In this case, the reaction was in its early stage and the cracks were not yet fully developed.

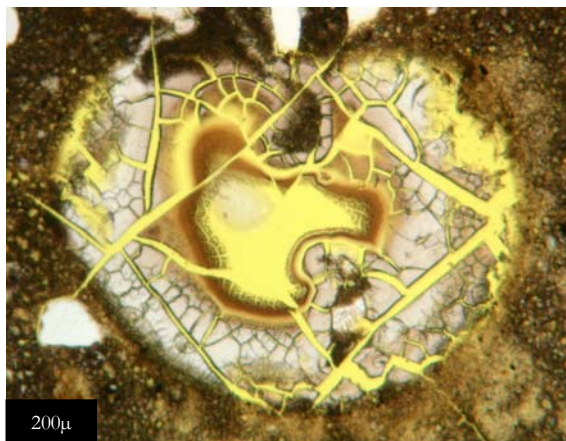


Figure 11: cracked alkali-silica gel infilling an air bubble. Plane polarized light.



Figure 12: cores of concrete containing alkali-reactive aggregates with reaction rims around.

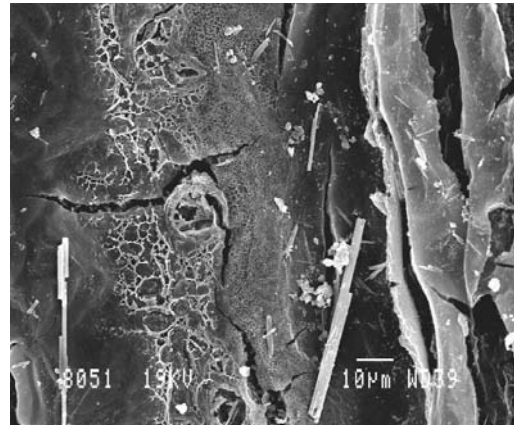


Figure 1 : superposition of alkali-silica gel layers.

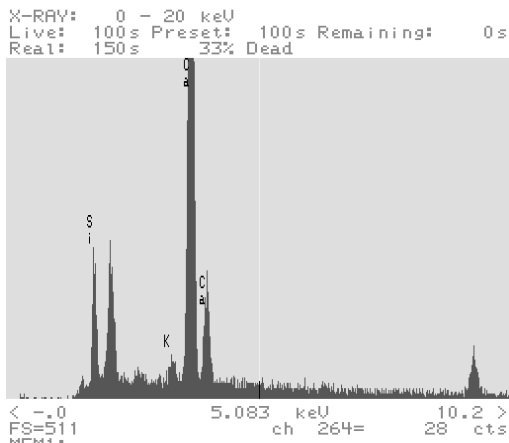


Figure 14: EDX spectrum of a K-rich alkali-silica gel.

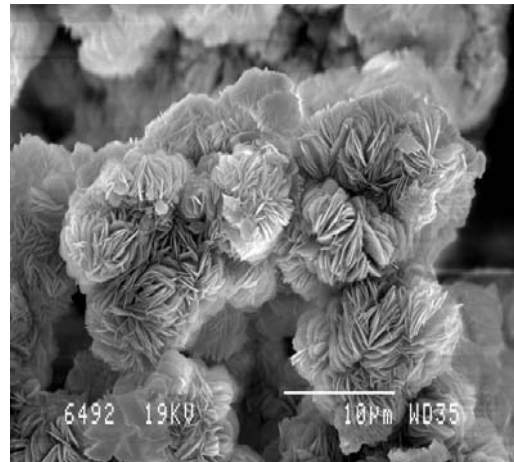


Figure 15: alkali-silica gel recrystallized in rosette-like minerals.

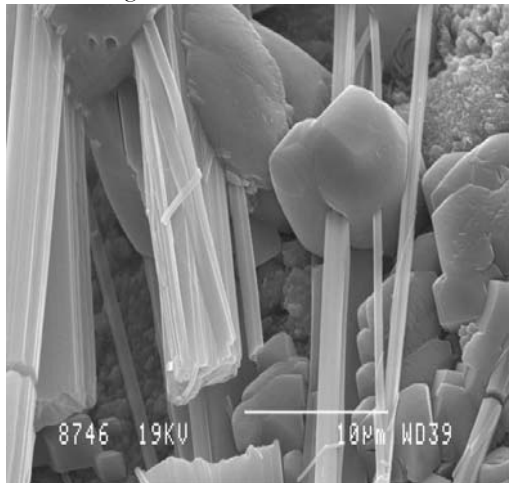


Figure 16: needle-like secondary ettringite minerals.

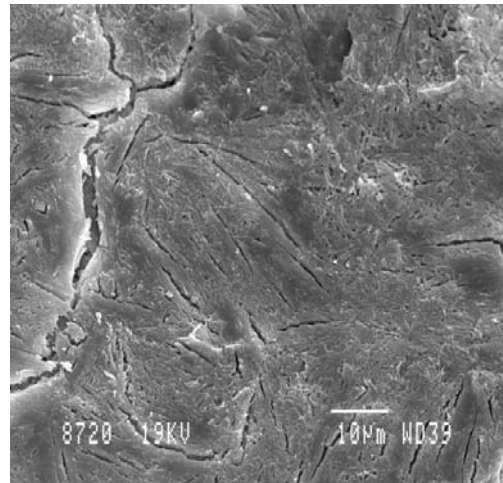


Figure 17: massive silica-ettringite with micro-cracks.